Occurrence of perfluoroalkyl substances in the Bay of Marseille (NW Mediterranean Sea) and the Rhône River

Natascha Schmidt, Vincent Fauvelle, Javier Castro-Jiménez, Katixa
Lajaunie-Salla, C. Pinazo, Christophe Yohia, Richard Sempere

▶ **To cite this version:**

HAL Id: hal-02265980

https://amu.hal.science/hal-02265980

Submitted on 13 Aug 2019

Occurrence of perfluoroalkyl substances in the Bay of Marseille (NW Mediterranean Sea) and the Rhône River

Natascha Schmidt[a], Vincent Fauvelle[a], Javier Castro-Jiménez[a],[*], Katixa Lajaunie-Salla[a], Christel Pinazo[a], Christophe Yohia[b], Richard Sempéré[a],[*]

[a] *Aix-Marseille Univ., Toulon Univ., CNRS, IRD, Mediterranean Institute of Oceanography (MIO), Marseille, France*
[b] *Aix-Marseille Univ., Toulon Univ., CNRS, IRD, OSU-Intitut Pytheas, Marseille, France*

ARTICLE INFO

ABSTRACT

Four perfluoroalkyl substances (PFAS) were analyzed in 62 duplicate surface water samples from the Rhône River and Marseille Bay (France; NW Mediterranean Sea). Perfluorooctane sulfonate (PFOS) was detected in all samples and exceeded the European Environmental Quality Standard (EQS) values in over 80% of the cases. The most contaminated samples were from the Rhône River (up to 200 ng L^{-1} Σ_4 PFAS), as well as those collected near a wastewater treatment plant outlet in Marseille Bay (up to 9 ng L^{-1} Σ_4 PFAS). While PFOS was the predominant PFAS in Marseille Bay, remarkably high concentrations of perfluorohexanoic acid (PFHxA) were measured in the Rhône River (8–193 ng L^{-1}). The relative abundances of individual compounds differed thus significantly between the Rhône River and Marseille Bay, indicating different sources. A simulation made with the MARS3D model showed that PFOS inputs from the Rhône River can enter Marseille Bay at levels > EQS.

1. Introduction

Perfluoroalkyl substances (PFAS) are a group of chemicals containing carbon-fluorine bonds, with varying perfluoroalkyl chain lengths. They show water and oil repellent properties and are used in a wide variety of application sectors: from textiles, inks and varnishes to firefighting foams (aqueous film forming foams, AFFFs) and for metal plating (Paul et al., 2009). They are also used as additives in pesticides (Sánchez-Avila et al., 2010). Perfluorooctane sulfonate (PFOS) is a widely used PFAS, which has been detected in freshwater and marine environments as well as in biota and humans (Earnshaw et al., 2014; Kärrman et al., 2007; Naile et al., 2010; Sánchez-Avila et al., 2010). Historically, the US enterprise 3 M™ was the main producer of PFOS, but in 2000 the company declared to phase PFOS out. Since the demand for PFOS and PFOS-related compounds remained high, this phase-out led to a dramatic increase in the production of these chemicals in China (Lim et al., 2011). PFOS has been identified as a Persistent Organic Pollutant (POP) and was thus included in the Annex B of the Stockholm Convention in 2010, leading to restrictions in use and production. While PFOS in the environment can originate directly from industrial production and consumer goods, it can also be the result of degradation of its precursors. PFOS-precursors are usually substituted perfluorooctyl sulfonamides and a high variety of structures and degradation pathways exists (Asher et al., 2012). Perfluorooctanoic acid (PFOA) is another highly persistent PFAS under natural conditions. In addition to historical uses, PFOA can be generated from degradation of long-chain fluorotelomer precursor types and perfluorooctane amide related compounds (Dasu et al., 2012; Mejia-Avendaño et al., 2016).

Growing evidence suggests toxicological effects of PFOS and PFOA on a variety of organisms (Hagenaars et al., 2008; Xia et al., 2014; Zhang et al., 2013). For example, it is suggested that PFOS exposure (depending on exposure time and concentration levels) can lead to epigenetic changes in sea urchins and affect the cardiac development in fish (Ding et al., 2015; Huang et al., 2011). Annual average Environmental Quality Standards (EQS) have thus been derived for biota (9.1 µg kg^{-1} biota wet weight), freshwater (0.00065 µg L^{-1}) and marine waters (0.00013 µg L^{-1}) in the European Union (Directive 2013/39/EU).

The Bay of Marseille in the NW Mediterranean Sea is subject to different anthropogenic pressures including touristic activity on the coastline (especially during high season in summer) recreational and commercial activities in the Old Harbor ("Vieux Port"), as well as ferry, leisure and commercial harbors (e.g., at L'Estaque). Additionally, the local wastewater treatment plant rejects from 0.4 to 3.8 m^3 s^{-1} wastewater (Oursel et al., 2013) into the sea at its outlet (Cortiou) eastwards of the city in the Calanques National Park. At Cortiou, the small rivers

[*] Corresponding authors.
E-mail addresses: javier.castro-jimenez@mio.osupytheas.fr (J. Castro-Jiménez), richard.sempere@mio.osupytheas.fr (R. Sempéré).

Huveaune and Jarret (1–5 m³ s⁻¹ and 0.5–3 m³ s⁻¹, respectively, Oursel et al., 2013) also enter the Mediterranean Sea, except during strong rain events, when the river water is deviated. The Bay of Marseille, and more generally the Gulf of Lions, is also subject to high solar radiation (Semperé et al., 2015) and strong wind regimes, which often make plant and plastic debris accumulate on the coast. Depending on wind forcing (among other factors), the Bay of Marseille can also be influenced by the Rhône River via freshwater intrusions (Fraysse et al., 2014; Gatti et al., 2006; Para et al., 2010).

The Rhône River is the main freshwater source of the Mediterranean Sea since the damming of the Nile River and a major carbon source (Semperé et al., 2000). It is 816 km long and has an average annual water discharge of 53×10^9 m³. The Rhône River has been strongly modified by human activities (e.g., dams, wastewater treatment plant inputs, hydro-electrical facilities) and has a history of polychlorinated biphenyls (PCB) contamination (Mourier et al., 2014). Recent studies also detected organic contaminants of emerging concern in its waters, such as phthalates and organophosphate esters (Paluselli et al., 2018; Schmidt et al., submitted), along with micro- and macroplastics (Castro-Jiménez et al., 2019; Schmidt et al., 2018). Furthermore, various PFAS have been found in aquatic plants, benthic invertebrates and different fish species from the Rhône River (Babut et al., 2017), and Miège et al. (2012) showed that more than two-thirds of fishes analyzed had PFOS concentrations above the EQS.

The objectives of this study were: (1) to investigate the waterborne occurrence of PFOS and three other PFAS (perfluorohexanoic acid - PFHxA, perfluorohexane sulfonic acid - PFHxS and perfluorooctanoic acid - PFOA) in the Rhône River and Marseille Bay; (2) to perform a local risk assessment by comparing the measured concentrations with the annual average EQS values for water and; (3) to investigate the PFOS inputs into the Gulf of Lions and the Bay of Marseille associated to freshwater intrusion from the Rhône River by using a modelling approach.

2. Materials & methods

2.1. Study area and sampling

Surface water samples (1 L) were collected from April 2017 to April 2018 in duplicate in the Rhône River at Arles city (n = 2 × 13) and at three sampling stations in Marseille Bay: L'Estaque harbor (n = 2 × 6), Frioul island (n = 2 × 6) and WWTP-Cortiou (n = 2 × 6) (Fig. 1) using a stainless steel collector, poured into corresponding 1 L glass bottles and filtered (GF/F, 0.7 μm retention size; Whatman, Maidstone, UK) within 3 h after collection and either stored at 4 °C in the dark and extracted within 24 h or otherwise stored at −25 °C until sample processing. River water temperature was measured using a handheld electronic thermometer whereas river flow data were extracted from "Banque Hydro" (http://www.hydro.eaufrance.fr/). The river flow data used originates from a measuring station in Tarascon, about 16 km upstream of Arles. Since the Rhône River divides into two branches downstream of the flow-measuring station, but upstream of the water sampling station, it was considered that the river flow at the water sampling station corresponds to about 90% (Semperé et al., 2000) of the flow measured in Tarascon.

2.2. Chemicals and standards

Hexane, dichloromethane and acetone (used to pre-clean the SPE cartridges) were purchased from Promochem (Picograde, LGC standard) together with ethyl acetate. Methanol was provided by Biosolve (ULC-MS grade), whereas ultrapure water was obtained from a Millipore (resistivity > 18.2 MΩ) Milli-Q system. Native PFAS were obtained from AccuStandard (USA) and isotope labeled PFAS (internal standards) from Wellington Laboratories (Canada). SPE glass cartridges were prepared in the laboratory using 250 mg hydrophilic-lipophilic

balance (HLB) Oasis ® (30 μm) bulk sorbent (Waters, Milford, USA).

2.3. Chemical analysis

Dissolved water phase samples were processed by solid phase extraction (SPE), using a method modified after Fauvelle et al. (2018) and analyzed for four PFAS (Fig. S1). Briefly, the filtrated water samples were vigorously shaken and passed through pre-cleaned glass cartridges using pre-cleaned polytetrafluoroethylene (PTFE) liners. Afterwards, 10 mL of ultrapure water were passed through the cartridges, which were then vacuum dried for 2 h. PFAS were eluted by using 5 mL of ethyl acetate followed by 5 mL of methanol. The extracts were then evaporated with pure N_2 gas until dryness and reconstituted using 990 μL methanol. Twenty ng sample⁻¹ of PFHxA-$^{13}C_5$ and PFOS-$^{13}C_8$ were added as internal standards. PFAS were quantified using a LC-QTOF (Agilent 1290 Infinity LC system coupled with Agilent 6530 Accurate-Mass Q-TOF, Agilent Technologies, Les Ulis, France). Separation was achieved using an Agilent Zorbax Eclipse XDB reversed phase column (50 mm × 2.1 mm, 1.8 μm), with temperature set at 30 °C. Quantification was performed using the isotope dilution method, considering the native analyte to internal standard area ratio and solvent-based calibration curves. Instrumental details are available in the Supplementary material (Text S1, Table S2).

Dissolved organic carbon (DOC) was measured from filtered (GF/F, 0.7 μm), acidified (by 20 μL of 85% H_3PO_4 acid) subsamples using a Shimadzu TOC-5000 carbon analyzer (Semperé et al., 2008). The instrument blank (≤5 μM) was subtracted from all measured results. All organic contaminant and DOC analysis were conducted in duplicate. The GF/F filters used for particulate organic carbon (POC) and nitrogen (PON) analysis were acidified with 50 μL H_2SO_4 (0.5 N) to remove inorganic carbon. POC and PON measurements were obtained using high combustion (1000 °C) on a CN Integra mass spectrometer (SERCON), calibrated using glycine references for every batch of 10–15 samples (Raimbault et al., 2008).

2.4. Quality assurance/quality control (QA/QC)

The whole procedure was conducted in an International Standards Organization (ISO) 6 cleanroom and strict QA/QC procedures were implemented. All glass materials and the GF/F filters were baked (450 °C, 6 h) prior to use. Given that PTFE might be a source of PFAS (at least at high temperatures; Schlummer et al. (2015)), its use was limited to SPE sample loading lines and each PFTE line was cleaned thoroughly with MeOH prior to use in order to avoid sample contamination. Replicate blanks were made during each extraction and no contamination was detected in any of the blanks. Method recoveries obtained during a previous method validation ranged from 73 ± 14 (PFHxS) to 124 ± 5 (PFOA)% (Fauvelle et al., 2018). Method limits of quantification ranged from 0.10 (PFOS) to 8.00 (PFHxA) ng L⁻¹. Concerning the linearity performance of the quantitative method, the linearity range was 0.5–200 ng mL⁻¹ for the calibration curve, the R^2 varied from 0.997 (PFHxS) to 0.999 (PFOS) and the slope RSD ranged from 2.3% (PFOS) to 5.1% (PFHxS). Samples were collected in duplicates and the concentrations of duplicates were averaged.

2.5. Hydrodynamic model (MARS3D)

The hydrodynamic model used to study the PFAS inputs from the Rhône River into the eastern Gulf of Lions was the three-dimensional MARS3D model (3D hydrodynamic Model for Applications at Regional Scale, IFREMER) as described in detail by Lazure and Dumas (2008). The high resolution MARS3D-RHOMA configuration was applied and validated for the simulation of oceanic circulation (Pairaud et al., 2011) and the biogeochemical processes of the Bay of Marseille by Fraysse et al. (2013) and was then used to reproduce realistic, observed conditions (Fraysse et al., 2014; Ross et al., 2016). The model domain
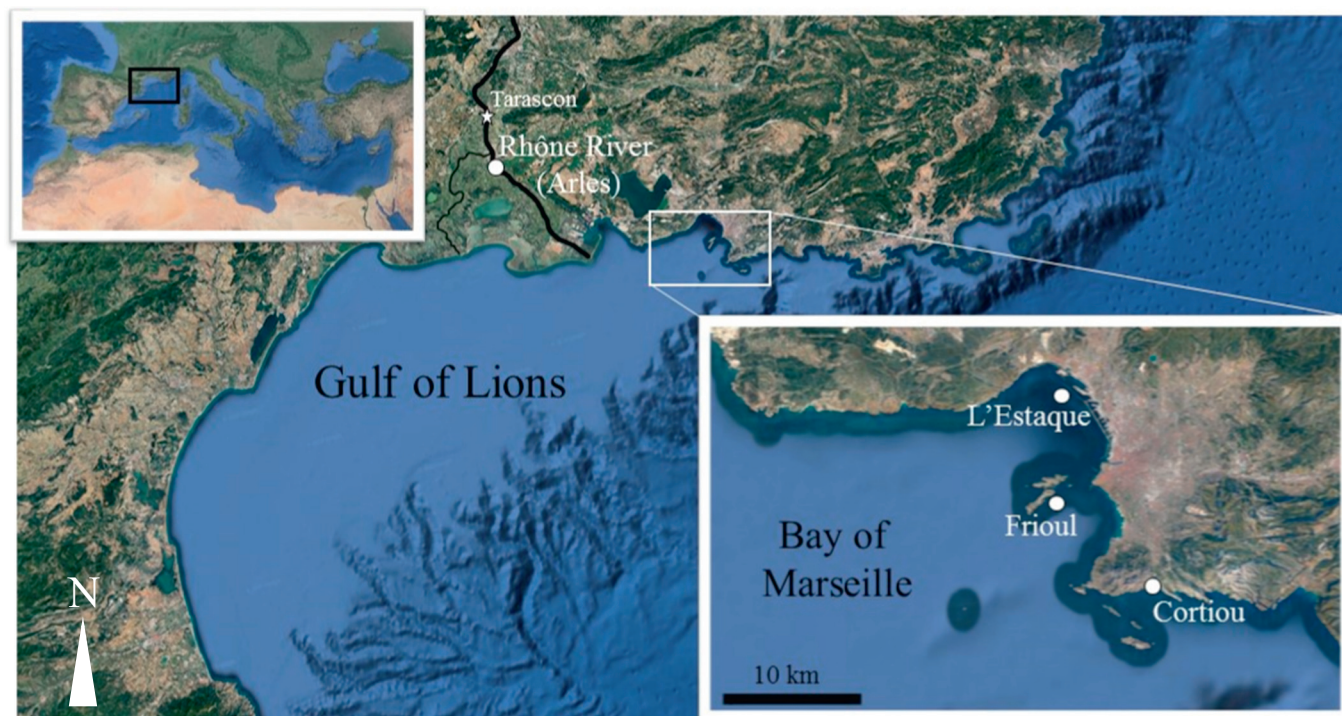
N. Schmidt, et al.

Fig. 1. Google Earth map of the study area in the Gulf of Lions (northwestern Mediterranean Sea, see upper left corner). The position of the river flow measuring station in the commune of Tarascon is indicated as well as the trace of the Rhône River and the sampling station in Arles city. A zoom of the Bay of Marseille (lower right corner) indicates the three marine sampling stations including L'Estaque harbor, Frioul island and WWTP-Cortiou.

covered an area of 100 km × 48 km between the mouth of the Rhône River and Cape Sicié (Fig. S2), with a horizontal resolution of 400 m and 30 sigma vertical levels. The model takes into account the forcing through the NW Mediterranean general circulation, on the basis of a nesting strategy with the large scale MARS3D-MENOR configuration (1.2 km resolution) (Nicolle et al., 2009). It is forced by the Rhône River discharge, and by atmospheric conditions of the year 2017, with a spatially homogenous wind reproducing the temporal evolution simulated at the SOLEMIO station in Marseille Bay (Fig. S2) thanks to the meteorological WRF-ARW model, which was described in detail by Klemp et al. (2007). The high resolution of the WRF-ARW configuration was applied for the atmospheric circulation and reproduced realistic conditions (Yohia, 2017). The model covers an area of 864 km by 1400 km with a resolution of 2 km and is forced by the GFS model (NCEP/NOAA).

The simulation was run for the year 2017 using inputs of PFAS concentrations measured in the Rhône River during field campaigns in between April 12th and December 12th (data from Table 1).

3. Results and discussion

3.1. Σ_4 PFAS concentrations and estimated flux to the Mediterranean Sea

Total PFAS concentrations were higher in the Rhône River (ranging from 13 to 200 ng L^{-1}) than in Marseille Bay (0.11–9 ng L^{-1}); the lowest concentration (0.11 ng L^{-1}) being detected in the Bay of Marseille (L'Estaque and Frioul stations; Table 1). Although the highest Σ_4 PFAS concentration observed in Marseille Bay was 9 ng L^{-1} near the Marseille-Cortiou-WWTP outlet, the concentrations were lower than those detected in the Rhône River. This could indicate that riverine sources are generally more important than coastal sources, that relatively low amounts of PFAS enter the WWTP, that an important dilution effect occurs after the wastewater enters the sea, or that the applied treatments efficiently remove important quantities of PFAS from the wastewater before releasing it into the sea. While it is difficult to clearly

Table 1

PFAS concentrations (in ng L^{-1}) measured in surface waters of the Rhône River and Marseille Bay. Asterisks indicate that the measured PFOS concentration exceeded the fresh- and seawater EQSs of 0.65 ng L^{-1} (Rhône River) or 0.13 ng L^{-1} (Cortiou, L'Estaque and Frioul).

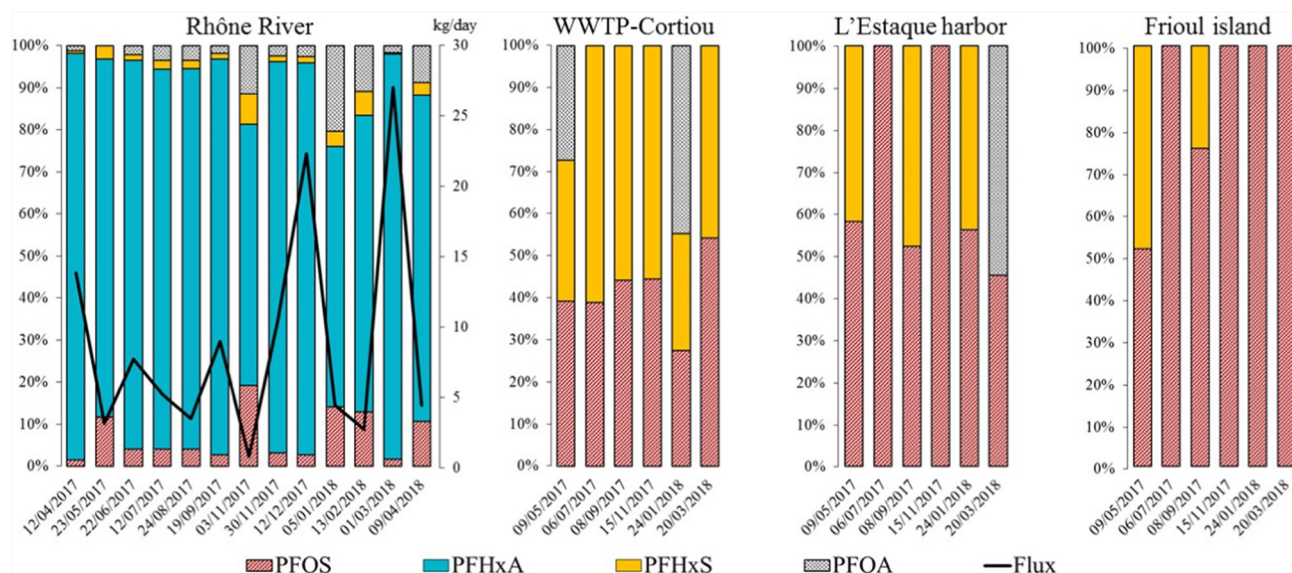| Station	Date	PFOS	PFHxA	PFHxS	PFOA	Σ
Rhône River	12/04/2017	2.97*	191	1.23	2.27	**198**
Rhône River	23/05/2017	3.68*	27	1.01	n.d.	**32**
Rhône River	22/06/2017	4.57*	104	1.60	2.32	**112**
Rhône River	12/07/2017	3.13*	69	1.58	2.68	**76**
Rhône River	24/08/2017	3.39*	76	1.67	2.92	**84**
Rhône River	19/09/2017	4.53*	154	2.23	3.10	**164**
Rhône River	03/11/2017	3.48*	11	1.33	2.06	**18**
Rhône River	30/11/2017	3.72*	108	1.54	2.81	**116**
Rhône River	12/12/2017	2.53*	87	1.41	2.35	**93**
Rhône River	05/01/2018	1.80*	8	0.47	2.58	**13**
Rhône River	13/02/2018	2.60*	14	1.14	2.19	**20**
Rhône River	01/03/2018	3.29*	193	0.63	3.21	**200**
Rhône River	09/04/2018	2.27*	17	0.63	1.87	**22**
Cortiou (WWTP outlet)	09/05/2017	3.44*	n.d.	2.93	2.38	**9**
Cortiou (WWTP outlet)	06/07/2017	1.79*	n.d.	2.80	n.d.	**4.6**
Cortiou (WWTP outlet)	08/09/2017	1.26*	n.d.	1.59	n.d.	**2.9**
Cortiou (WWTP outlet)	15/11/2017	1.68*	n.d.	2.10	n.d.	**3.8**
Cortiou (WWTP outlet)	24/01/2018	1.52*	n.d.	1.53	2.46	**5.5**
Cortiou (WWTP outlet)	20/03/2018	1.02*	< LOQ	0.86	n.d.	**1.9**
L'Estaque harbor	09/05/2017	0.25*	n.d.	0.18	n.d.	**0.43**
L'Estaque harbor	06/07/2017	0.12	n.d.	n.d.	n.d.	**0.12**
L'Estaque harbor	08/09/2017	0.16*	n.d.	0.15	n.d.	**0.31**
L'Estaque harbor	15/11/2017	0.11	n.d.	n.d.	n.d.	**0.11**
L'Estaque harbor	24/01/2018	0.17*	n.d.	0.14	n.d.	**0.31**
L'Estaque harbor	20/03/2018	0.15*	n.d.	n.d.	0.18	**0.33**
Frioul island	09/05/2017	0.16*	n.d.	0.15	n.d.	**0.31**
Frioul island	06/07/2017	0.11	n.d.	n.d.	n.d.	**0.11**
Frioul island	08/09/2017	0.45*	n.d.	0.14	n.d.	**0.59**
Frioul island	15/11/2017	0.12	n.d.	n.d.	n.d.	**0.12**
Frioul island	24/01/2018	0.12	n.d.	n.d.	n.d.	**0.12**
Frioul island	20/03/2018	0.35*	n.d.	n.d.	n.d.	**0.35**

Fig. 2. Relative abundances (in %) of the four PFAS at each sampling date at the four sites. For the Rhône River, the black line indicates the estimated daily flux (in kg day^{-1}) of Σ_4 PFAS into the Mediterranean Sea.

name the source of the high PFAS concentrations detected in the Rhône River, one possible explanation could be the textile industry. PFAS are commonly used for technical and outdoor clothing, and the Rhône-Alpes region is leading the French textile industry with 712 companies and > 15,000 workers (UNITEX, http://medef-aura.fr/rhone-alpes-premiere-region-textile-francaise.html).

To roughly estimate the flux of PFAS into the NW Mediterranean Sea, the measured concentrations of each sampling event were multiplied with the corresponding daily river discharge. The estimated daily dissolved water phase Σ_4 PFAS flux from the Rhône River into the Mediterranean Sea varies thus between 0.72 and 27 kg day^{-1} (Fig. 2). The high variability results hereby from the high variability in measured PFAS concentrations and the high temporal fluctuations of the river discharge (between 460 and 3960 m^3 s^{-1} on sampling events). While the river discharge had important temporal fluctuations, we counted six sampling events with a discharge < 1000 m^3 s^{-1} and seven sampling events with a discharge > 1000 m^3 s^{-1} (three of which were > 2000 m^3 s^{-1}), indicating a relatively good equilibrium of samples taken in situations of low and high water discharge. Still, the calculated flux can only be considered as a limited, rough estimation, but it gives a first idea of PFAS inputs from the dissolved phase of the Rhône River to the Mediterranean Sea. For individual compounds we calculated fluxes of 4.13–18 kg month^{-1} (PFOS), 2.45–27 kg month^{-1} (PFOA; not taking into account the one sampling date when PFOA was not detected), 13–783 kg month^{-1} (PFHxA) and 1.59–10 kg month^{-1} (PFHxS) when considering one month as equal to 30 days.

3.2. Relative abundances of individual compounds

In the Rhône River, the predominant compound was PFHxA, with its relative abundance varying between 62 and 97%, while PFHxS was the least abundant compound with < 1–7%. PFOS made up for 2–19% of the sample composition in the Rhône River. Interestingly, Miège et al. (2012) did not detect any PFHxA in their fish samples from the Rhône River (PFOS was most abundant in their samples), indicating that the relative abundances of PFAS in biota and water samples can be very different, possibly due to the different bioaccumulation potential of individual PFAS, in relation to their different perfluoroalkyl chain length (Simmonet-Laprade et al., 2019). In contrast, in Marseille Bay PFOS was generally dominating the PFAS composition with 16–54% (WWTP-Cortiou), 45–100% (L'Estaque harbor) and 52–100% (Frioul

island). Furthermore, PFHxS had sometimes a relatively high relative abundance with 14–61% in WWTP-Cortiou and 0–48% in L'Estaque and Frioul stations. PFOA was never detected in Frioul, once in L'Estaque station (with 55% relative abundance) and twice in WWTP-Cortiou (27% and 45% relative abundance). In the Rhône River PFOA abundance varied between 0 and 20% (Fig. 2). These results clearly indicate net differences in the relative abundance of PFAS in waters from Marseille Bay and the Rhône River, suggesting different sources and/or environmental processes. Moreover, WWTP-Cortiou exhibits a different pattern than the other two marine stations, with higher Σ_4 PFAS concentrations and differing relative abundances (lower PFOS abundance; PFHxS abundance always > 0). This is probably due to specific WWTP related PFAS inputs at the WWTP outlet, but it also indicates that Σ_4 PFAS compound composition can be variable at a small spatial scale and that the WWTP outlet does not necessarily have an influence on PFAS occurrence and abundance in the inner Bay of Marseille, even though this needs further investigations.

In the riverine samples, PFHxA was found at concentrations of 8–193 ng L^{-1} (Table 1). Our maximum PFHxA concentration detected is about 20 times higher than the one observed in the Danube River by Loos et al. (2017) (max. 8.5 ng L^{-1}) and more than two-fold the highest amount measured by Munoz et al. (2015) during a French nationwide survey comprising 333 freshwater samples (max. 86 ng L^{-1}). However, in accordance with our results, Munoz et al. (2015) observed that PFHxA concentrations in the Rhône River were very variable and could reach higher relative abundances than in other watersheds. The authors suggested that the high PFHxA amounts could hereby originate from a fluorochemical plant producing polyvinylidene fluoride. This factory is located over 250 km upstream of our sampling station, but given the persistence of PFAS (Kunacheva et al., 2011; Stahl et al., 2011) and the high mobility of short-chain perfluorocarboxylates (Ateia et al., 2019), it could still be a possible explanation for the high PFHxA concentrations measured in this study. In a Mediterranean wetland area, up to 18.7 ng L^{-1} of PFHxA have been detected (Lorenzo et al., 2019). In Marseille Bay, PFHxA was only detected once (at a concentration < LOQ) at WWTP-Cortiou station, where some freshwater inputs occur via the rivers Huveaune and Jarret. We thus suggest that high PFHxA concentrations could possibly be considered as a tracer of a riverine signature. This is in accordance with previous observations in the Atlantic Ocean where PFHxA was only detected in samples closest to the Amazon River mouth (Schmidt et al., 2019).
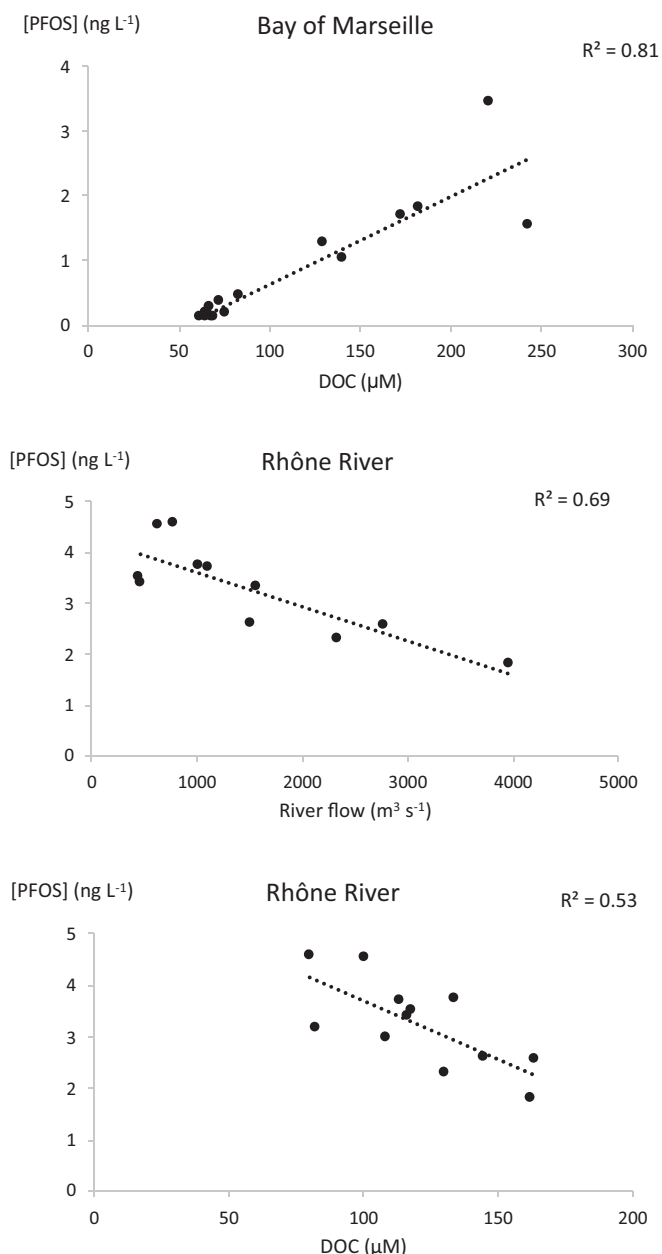
[PFOS] (ng L⁻¹)

Bay of Marseille

R² = 0.81

DOC (µM)

[PFOS] (ng L⁻¹)

Rhône River

R² = 0.69

River flow (m³ s⁻¹)

[PFOS] (ng L⁻¹)

Rhône River

R² = 0.53

DOC (µM)

Fig. 3. Relationships between PFOS concentrations and DOC (Bay of Marseille, Rhône River) or river discharge (Rhône River).

3.3. PFOS occurrence, estimated flux and modelled inputs to Marseille Bay via freshwater intrusions

PFOS was detected in all seawater and freshwater samples. In the Bay of Marseille, PFOS and DOC concentrations were positively correlated (p-value < 0.001), as has been observed before in seawater of the North Sea (Ahrens et al., 2009). In the Rhône River, PFOS concentrations seem mainly driven by the magnitude of river discharge (p-value = 0.002). However, DOC and POC concentrations are well correlated with river discharge (see Table S1 for all DOC, POC, PON and river discharge data), PFOS is also correlated with DOC in the Rhône River (p-value = 0.007). Hereby, the correlation is negative (i.e., an increase in DOC entrains a decrease in PFOS concentrations), in contrast to the correlation observed between DOC and PFOS in seawater samples from Marseille Bay (Fig. 3). The negative correlation between PFOS and river flowrate might indicate that the PFOS sources in the Rhône River are rather constant and the PFOS amounts are more or less

diluted depending on the river discharge. Another explanation could be that the increased amount of suspended particulate matter (such as POC) during high river discharge might enhance the sequestration of long-chain PFAS and thus reduce the dissolved PFOS concentration.

In this study, 84% of samples had PFOS concentrations higher than the respective annual average (AA) EQS (i.e., 0.65 ng L⁻¹ for freshwater and 0.13 ng L⁻¹ for marine waters). All samples from the Rhône River and Cortiou station showed concentrations ∼ 3–7 or ∼8–26 times higher than the corresponding AA EQS, respectively. At L'Estaque station, 67% of samples had exceeding PFOS concentrations, whereas this was the case for only 50% of samples from Frioul station (Table 1). The Maximum Allowable Concentration (MAC) EQS for PFOS (36,000 ng L⁻¹ in freshwater and 7200 ng L⁻¹ in marine waters) was never exceeded in our study. A recent study showed that some invertebrates (Oligochaetes and Dytiscidae) and fish samples from the Rhône River also exhibited PFOS concentrations exceeding the EQS (EQS$_{biota}$ of 9.1 µg kg⁻¹), with up to 27 µg kg⁻¹ detected (Babut et al., 2017). It thus seems as if the Rhône River food web could be affected by the environmental PFOS contamination and potentially negative impacts on human health through fish consumption should be investigated. The highest PFOS concentration measured in this study was on 22/06/2017 in the Rhône River (4.6 ng L⁻¹), where 1.8 ng L⁻¹ was the lowest concentration observed (on 05/01/2018). These values are comparable to those of the River Rhine upstream of Leverkusen in Germany (1.41–6.38 ng L⁻¹, Möller et al., 2010) and Swedish Rivers (0.04–6.90 ng L⁻¹, Nguyen et al., 2017) as well as those of three samples collected in the Rhône River in 2012 (1.5–4.9 ng L⁻¹, Munoz et al., 2015). Significantly higher PFOS concentrations of 36.3–703.3 ng L⁻¹ were measured in the Yangtze River Estuary in China (Pan and You, 2010).

Using the PFOS concentrations measured and the corresponding daily river discharge, a PFOS input from the Rhône River into the Mediterranean Sea of 138–616 (mean 338, median 330) g day⁻¹ was estimated. For comparison, we made the same calculation using data from Lorenzo et al. (2016) and Loos et al. (2008) (mean PFOS concentrations 2.2 ng L⁻¹ and 5.55 ng L⁻¹, respectively) together with the average water discharges of the Ebro and Po Rivers (426 m³ s⁻¹ and 1540 m³ s⁻¹, respectively) and obtained a daily PFOS input into the Mediterranean Sea of 81 g from the Ebro River and 738 g from the Po River. However, the comparison with the Po River has restrictions, since the authors did not filter their water samples prior to analysis, in contrast to this study and the one from Lorenzo et al. (2016). The Ebro River is, by drainage basin, the third largest river flowing into the Mediterranean Sea, but its discharge is restrained due to high water demands (Lorenzo et al., 2016; Struglia et al., 2004). For comparison, the Nile River has an average discharge of approximately 1200 m³ s⁻¹ (Struglia et al., 2004), but its drainage basin is by far the largest of all the rivers draining into the Mediterranean Sea (2.988 × 10⁶ km², compared to 0.098 × 10⁶ km² for the Rhône River) (Montreuil and Ludwig, 2013). To get a better idea concerning global riverine PFOS inputs into the Mediterranean Sea, it would thus be important to obtain measurement data from the Nile River, as well.

The numerical approach chosen to investigate the PFOS inputs from the Rhône River into the eastern part of the Gulf of Lions allowed us to examine whether the Bay of Marseille is influenced by these inputs or not. Hereby, the simulation started on 01/01/2017 and the contaminants were injected continually with concentrations punctually updated at the dates for which measurement data was available, and with an interpolation between two dates. The temporal series (Fig. S3) indicate that in the Bay of Marseille, the first PFAS inputs originating from the Rhône River were perceivable at the beginning of October 2017 in L'Estaque and Frioul stations and approximately one month later - at much lower concentrations - in WWTP-Cortiou, which is farther away from the source and is rather protected from currents through the neighboring cliffs. In the vicinity of the Rhône River mouth, the modelled PFOS concentrations were quite high (≥1 ng L⁻¹);
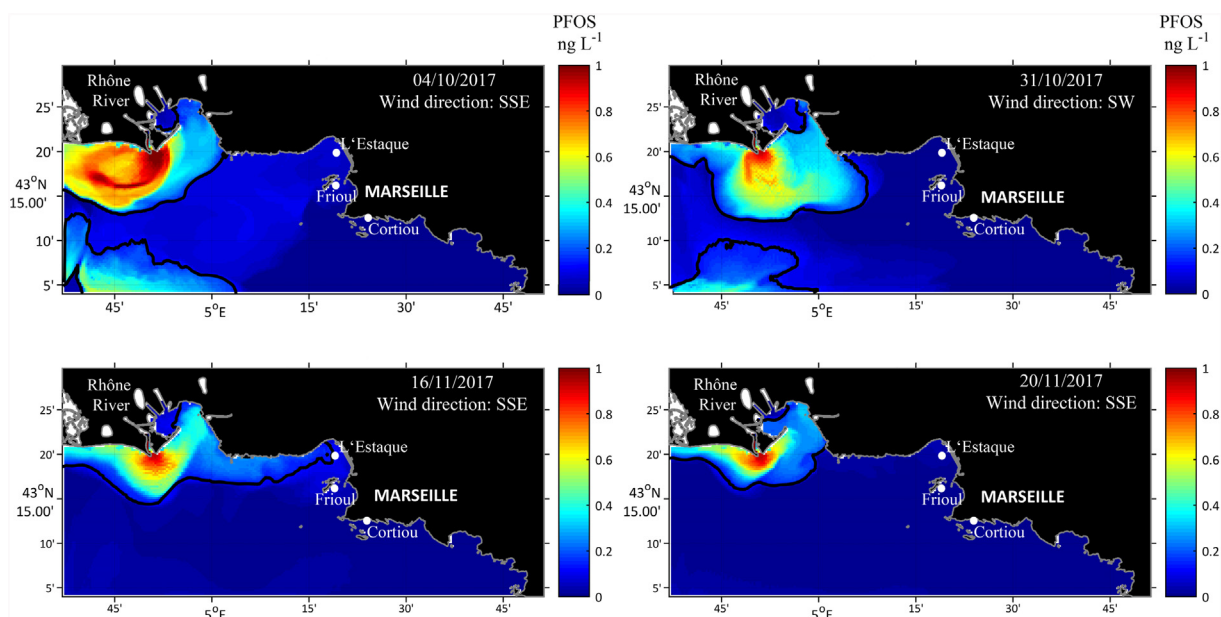
Fig. 4. Simulated PFOS distribution (with concentrations in ng L^{-1}) in the eastern part of the Gulf of Lions, including the Rhône River mouth and the Bay of Marseille. The black isoline indicates a PFOS concentration of 0.13 ng L^{-1}, the EQS for marine waters. Four dates were chosen to represent different directions and extensions of the river plume. The color bar is limited between 0 and 1 ng L^{-1} to better represent low concentrations (including the EQS value of 0.13 ng L^{-1}); note that dark red values can also represent concentrations > 1 ng L^{-1}. (For interpretation of the references to color in this figure legend, the reader is referred to the web version of this article.)

negative effects on the aquatic food web in and near the estuary can thus not be excluded and require further investigations. Furthermore, even in the northern part of the Bay of Marseille (e.g., in L'Estaque), the PFOS input from the Rhône River is sometimes enough to exceed the EQS value (EQS of 0.13 ng L^{-1}; see black isoline in Fig. 4) in these marine waters (Fig. 4). The maximum value simulated at l'Estaque on November 16th occurred during south-south-easterly winds, associated with the anticyclonic Marseille eddy, which is necessary to advect the diluted Rhône River waters toward the northern part of the Bay (Fraysse et al., 2014). In contrast the south-westerly winds that occurred for example on October 31st moved the panache eastwards without generating the eddy necessary to reach the Bay of Marseille. Maps of the barotropic currents for the four selected dates from Fig. 4 can be found in the Supplementary material (Fig. S4).

4. Conclusion

Highest PFAS concentrations were detected in the Rhône River, followed by WWTP-Cortiou and the two other marine sampling stations. Relative abundances of individual compounds between samples from the Rhône River and Marseille Bay were strongly different, probably indicating different PFAS sources. PFOS concentrations were exceeding the annual average EU EQS values in over 80% of samples. As shown by our results and comparison with literature, PFOS concentrations exceeding the EQS seems to be a frequent situation and should encourage decision makers to enforce stricter measures to avoid and reduce the contamination of water bodies. While at Cortiou station the local WWTP and/or riverine inputs through the Huveaune and Jarret rivers are the most likely PFOS sources, the model simulation indicated that in L'Estaque station the exceeding PFOS concentrations could – at least partly – result from inputs from the Rhône River. Our data furthermore suggest that up to 27 kg of dissolved water phase Σ_4 PFAS could enter the Gulf of Lion area in the Mediterranean Sea each day through freshwater inputs from the Rhône River. This points to the Rhône River as a possible major source of PFAS to the Mediterranean Sea and a monitoring with higher spatial and temporal resolution is needed to validate our observations. Model results could be improved

by considering heterogeneous atmospheric conditions to better represent upwelling and river intrusion events.

References

Ahrens, L., Felizeter, S., Ebinghaus, R., 2009. Spatial distribution of polyfluoroalkyl compounds in seawater of the German Bight. Chemosphere 76, 179–184. https://doi.org/10.1016/j.chemosphere.2009.03.052.

Asher, B.J., Wang, Y., De Silva, A.O., Backus, S., Muir, D.C.G., Wong, C.S., Martin, J.W., 2012. Enantiospecific perfluorooctane sulfonate (PFOS) analysis reveals evidence for the source contribution of PFOS-precursors to the Lake Ontario foodweb. Environ. Sci. Technol. 46, 7653–7660. https://doi.org/10.1021/es301160r.

Ateia, M., Maroli, A., Tharayil, N., Karanfil, T., 2019. The overlooked short- and ultra-short-chain poly- and perfluorinated substances: a review. Chemosphere 220, 866–882. https://doi.org/10.1016/j.chemosphere.2018.12.186.

Babut, M., Labadie, P., Simonnet-Laprade, C., Munoz, G., Roger, M.C., Ferrari, B.J.D., Budzinski, H., Sivade, E., 2017. Per- and poly-fluoroalkyl compounds in freshwater fish from the Rhône River: influence of fish size, diet, prey contamination and bio-transformation. Sci. Total Environ. 605–606, 38–47. https://doi.org/10.1016/j.scitotenv.2017.06.111.

Castro-Jiménez, J., González-Fernández, D., Fornier, M., Schmidt, N., Sempéré, R., 2019. Macro-litter in surface waters from the Rhone River: plastic pollution and flows to the NW Mediterranean Sea. Mar. Pollut. Bull. 146, 60–66. https://doi.org/10.1016/j.

marpolbul.2019.05.067.

Dasu, K., Liu, J., Lee, L.S., 2012. Aerobic soil biodegradation of 8:2 fluorotelomer stearate monoester. Environ. Sci. Technol. 46, 3831–3836. https://doi.org/10.1021/es203978g.

Ding, G., Wang, L., Zhang, J., Wei, Y., Wei, L., Li, Y., Shao, M., Xiong, D., 2015. Toxicity and DNA methylation changes induced by perfluorooctane sulfonate (PFOS) in sea urchin Glyptocidaris crenularis. Chemosphere 128, 225–230. https://doi.org/10.1016/j.chemosphere.2015.01.045.

Earnshaw, M.R., Paul, A.G., Loos, R., Tavazzi, S., Paracchini, B., Scheringer, M., Hungerbühler, K., Jones, K.C., Sweetman, A.J., 2014. Comparing measured and modelled PFOS concentrations in a UK freshwater catchment and estimating emission rates. Environ. Int. 70, 25–31. https://doi.org/10.1016/j.envint.2014.05.004.

Fauvelle, V., Castro-Jiménez, J., Schmidt, N., Carlez, B., Panagiotopoulos, C., Sempéré, R., 2018. One-single extraction procedure for the simultaneous determination of a wide range of polar and nonpolar organic contaminants in seawater. Front. Mar. Sci. 5, 1–10. https://doi.org/10.3389/fmars.2018.00295.

Fraysse, M., Pinazo, C., Faure, V.M., Fuchs, R., Lazzari, P., Raimbault, P., Pairaud, I., 2013. Development of a 3D coupled physical-biogeochemical model for the Marseille Coastal Area (NW Mediterranean Sea): what complexity is required in the coastal zone? PLoS One 8. https://doi.org/10.1371/journal.pone.0080012.

Fraysse, M., Pairaud, I., Ross, O.N., Faure, V.M., Pinazo, C., 2014. Intrusion of Rhone River diluted water into the Bay of Marseille: generation processes and impacts on ecosystem functioning. J. Geophys. Res. Oceans 119, 6535–6556. https://doi.org/10.1002/2014JC010022.Received.

Gatti, J., Petrenko, A., Devenon, J.L., Leredde, Y., Ulses, C., 2006. The Rhone river dilution zone present in the northeastern shelf of the Gulf of Lion in December 2003. Cont. Shelf Res. 26, 1794–1805. https://doi.org/10.1016/j.csr.2006.05.012.

Hagenaars, A., Knapen, D., Meyer, I.J., van der Ven, K., Hoff, P., De Coen, W., 2008. Toxicity evaluation of perfluorooctane sulfonate (PFOS) in the liver of common carp (Cyprinus carpio). Aquat. Toxicol. 88, 155–163. https://doi.org/10.1016/j.aquatox.2008.04.002.

Huang, Q., Fang, C., Wu, X., Fan, J., Dong, S., 2011. Perfluorooctane sulfonate impairs the cardiac development of a marine medaka (Oryzias melastigma). Aquat. Toxicol. 105, 71–77. https://doi.org/10.1016/j.aquatox.2011.05.012.

Kärrman, A., Langlois, I., Bavel, B. van, Lindström, G., Oehme, M., 2007. Identification and pattern of perfluorooctane sulfonate (PFOS) isomers in human serum and plasma. Environ. Int. 33, 782–788. https://doi.org/10.1016/j.envint.2007.02.015.

Klemp, J.B., Skamarock, W.C., Dudhia, J., 2007. Conservative split-explicit time integration methods for the compressible nonhydrostatic equations. Mon. Weather Rev. 135, 2897–2913. https://doi.org/10.1175/MWR3440.1.

Kunacheva, C., Senevirathna, S.T.M.L.D., Tanaka, S., Fujii, S., Lien, N.P.H., Nozoe, M., Shivakoti, B.R., 2011. The emergence of persistent organic pollutants in the environment: the occurrence and treatment of perfluorinated compounds. SANSAI An Environ. J. Glob. Community 5, 37–50.

Lazure, P., Dumas, F., 2008. An external-internal mode coupling for a 3D hydrodynamical model for applications at regional scale (MARS). Adv. Water Resour. 31, 233–250. https://doi.org/10.1016/j.advwatres.2007.06.010.

Lim, T.C., Wang, B., Huang, J., Deng, S., Yu, G., 2011. Emission inventory for PFOS in China: review of past methodologies and suggestions. ScientificWorldJournal 11, 1963–1980. https://doi.org/10.1100/2011/868156.

Loos, R., Locoro, G., Huber, T., Wollgast, J., Christoph, E.H., de Jager, A., Manfred Gawlik, B., Hanke, G., Umlauf, G., Zaldívar, J.M., 2008. Analysis of perfluorooctanoate (PFOA) and other perfluorinated compounds (PFCs) in the River Po watershed in N-Italy. Chemosphere 71, 306–313. https://doi.org/10.1016/j.chemosphere.2007.09.022.

Loos, R., Tavazzi, S., Mariani, G., Suurkuusk, G., Paracchini, B., Umlauf, G., 2017. Analysis of emerging organic contaminants in water, fish and suspended particulate matter (SPM) in the Joint Danube Survey using solid-phase extraction followed by UHPLC-MS-MS and GC–MS analysis. Sci. Total Environ. 607–608, 1201–1212. https://doi.org/10.1016/j.scitotenv.2017.07.039.

Lorenzo, M., Campo, J., Farré, M., Pérez, F., Picó, Y., Barceló, D., 2016. Perfluoroalkyl substances in the Ebro and Guadalquivir river basins (Spain). Sci. Total Environ. 540, 191–199. https://doi.org/10.1016/j.scitotenv.2015.07.045.

Lorenzo, M., Campo, J., Morales Suárez-Varela, M., Picó, Y., 2019. Occurrence, distribution and behavior of emerging persistent organic pollutants (POPs) in a Mediterranean wetland protected area. Sci. Total Environ. 646, 1009–1020. https://doi.org/10.1016/j.scitotenv.2018.07.304.

Mejia-Avendaño, S., Duy, S.V., Sauvé, S., Liu, J., 2016. Generation of perfluoroalkyl acids from aerobic biotransformation of quaternary ammonium polyfluoroalkyl surfactants. Environ. Sci. Technol. 50, 9923–9932. https://doi.org/10.1021/acs.est.6b00140.

Miège, C., Peretti, A., Labadie, P., Budzinski, H., Le Bizec, B., Vorkamp, K., Tronczynski, J., Persat, H., Coquery, M., Babut, M., 2012. Occurrence of priority and emerging organic compounds in fishes from the Rhone River (France). Anal. Bioanal. Chem. 404, 2721–2735. https://doi.org/10.1007/s00216-012-6187-0.

Möller, A., Ahrens, L., Surm, R., Westerveld, J., Van Der Wielen, F., Ebinghaus, R., De Voogt, P., 2010. Distribution and sources of polyfluoroalkyl substances (PFAS) in the River Rhine watershed. Environ. Pollut. 158, 3243–3250. https://doi.org/10.1016/j.envpol.2010.07.019.

Montreuil, O., Ludwig, W., 2013. Rivers of the Mediterrenean Sea: water discharge and nutrient fluxes. UNEP MED POL 1–126.

Mourier, B., Desmet, M., Van Metre, P.C., Mahler, B.J., Perrodin, Y., Roux, G., Bedell, J.P., Lefèvre, I., Babut, M., 2014. Historical records, sources, and spatial trends of PCBs along the RhÔne River (France). Sci. Total Environ. 476–477, 568–576. https://doi.org/10.1016/j.scitotenv.2014.01.026.

Munoz, G., Giraudel, J.L., Botta, F., Lestremau, F., Dévier, M.H., Budzinski, H., Labadie, P., 2015. Spatial distribution and partitioning behavior of selected poly- and perfluoroalkyl substances in freshwater ecosystems: a French nationwide survey. Sci. Total Environ. 517, 48–56. https://doi.org/10.1016/j.scitotenv.2015.02.043.

Naile, J.E., Khim, J.S., Wang, T., Chen, C., Luo, W., Kwon, B.O., Park, J., Koh, C.H., Jones, P.D., Lu, Y., Giesy, J.P., 2010. Perfluorinated compounds in water, sediment, soil and biota from estuarine and coastal areas of Korea. Environ. Pollut. 158, 1237–1244. https://doi.org/10.1016/j.envpol.2010.01.023.

Nguyen, M.A., Wiberg, K., Ribeli, E., Josefsson, S., Futter, M., Gustavsson, J., Ahrens, L., 2017. Spatial distribution and source tracing of per- and polyfluoroalkyl substances (PFASs) in surface water in Northern Europe. Environ. Pollut. 220, 1438–1446. https://doi.org/10.1016/j.envpol.2016.10.089.

Nicolle, A., Garreau, P., Liorzou, B., 2009. Modelling for anchovy recruitment studies in the Gulf of Lions (Western Mediterranean Sea). Ocean Dyn. 59, 953–968. https://doi.org/10.1007/s10236-009-0221-6.

Oursel, B., Garnier, C., Durrieu, G., Mounier, S., Omanović, D., Lucas, Y., 2013. Dynamics and fates of trace metals chronically input in a Mediterranean coastal zone impacted by a large urban area. Mar. Pollut. Bull. 69, 137–149. https://doi.org/10.1016/j.marpolbul.2013.01.023.

Pairaud, I.L., Gatti, J., Bensoussan, N., Verney, R., Garreau, P., 2011. Hydrology and circulation in a coastal area off Marseille: validation of a nested 3D model with observations. J. Mar. Syst. 88, 20–33. https://doi.org/10.1016/j.jmarsys.2011.02.010.

Paluselli, A., Aminot, Y., Galgani, F., Net, S., Sempéré, R., 2018. Occurrence of phthalate acid esters (PAEs) in the northwestern Mediterranean Sea and the Rhone River. Prog. Oceanogr. 163, 221–231. https://doi.org/10.1016/j.pocean.2017.06.002.

Pan, G., You, C., 2010. Sediment-water distribution of perfluorooctane sulfonate (PFOS) in Yangtze River Estuary. Environ. Pollut. 158, 1363–1367. https://doi.org/10.1016/j.envpol.2010.01.011.

Para, J., Coble, P.G., Charrière, B., Tedetti, M., Fontana, C., Sempéré, R., 2010. Fluorescence and absorption properties of chromophoric dissolved organic matter (CDOM) in coastal surface waters of the northwestern Mediterranean Sea, influence of the Rhône River. Biogeosciences 7, 4083–4103. https://doi.org/10.5194/bg-7-4083-2010.

Paul, A.G., Jones, K.C., Sweetman, A.J., 2009. A First Global Production, Emission, And Environmental Inventory For Perfluorooctane Sulfonate. Environ. Sci. Technol. 43 (2), 386–392.

Raimbault, P., Garcia, N., Cerutti, F., 2008. Distribution of inorganic and organic nutrients in the South Pacific Ocean — evidence for long-term accumulation of organic matter in nitrogen-depleted waters. Biogeosciences 5, 281–298. https://doi.org/10.5194/bg-5-281-2008.

Ross, O.N., Fraysse, M., Pinazo, C., Pairaud, I., 2016. Impact of an intrusion by the Northern Current on the biogeochemistry in the eastern Gulf of Lion, NW Mediterranean. Estuar. Coast. Shelf Sci. 170, 1–9. https://doi.org/10.1016/j.ecss.2015.12.022.

Sánchez-Avila, J., Meyer, J., Lacorte, S., 2010. Spatial distribution and sources of perfluorochemicals in the NW Mediterranean coastal waters (Catalonia, Spain). Environ. Pollut. 158, 2833–2840. https://doi.org/10.1016/j.envpol.2010.06.022.

Schlummer, M., Sölch, C., Meisel, T., Still, M., Gruber, L., Wolz, G., 2015. Emission of perfluoroalkyl carboxylic acids (PFCA) from heated surfaces made of polytetrafluoroethylene (PTFE) applied in food contact materials and consumer products. Chemosphere 129, 46–53. https://doi.org/10.1016/j.chemosphere.2014.11.036.

Schmidt, N., Thibault, D., Galgani, F., Paluselli, A., Sempéré, R., 2018. Occurrence of microplastics in surface waters of the Gulf of Lion (NW Mediterranean Sea). Prog. Oceanogr. 163, 214–220. https://doi.org/10.1016/j.pocean.2017.11.010.

Schmidt, N., Fauvelle, V., Ody, A., Castro-Jiménez, J., Jouanno, J., Changeux, T., Thibaut, T., Sempéré, R., 2019. The Amazon River – a major source of organic plastic additives to the tropical North Atlantic? Environ. Sci. Technol. https://doi.org/10.1021/acs.est.9b01585.

Schmidt, N., Castro-Jiménez, J., Fauvelle, V., Ourgaud, M., Sempéré, R., n.d. Occurrence of organic plastic additives in surface waters of the Rhône River (France). Environ. Pollut. (submitted).

Sempéré, R., Charrière, B., Van Wambeke, F., Cauwet, G., 2000. Carbon inputs of the Rhône River to the Mediterranean Sea: biogeochemical implications. Glob. Biogeochem. Cycles 14, 669–681. https://doi.org/10.1029/1999GB900069.

Sempéré, R., Tedetti, M., Panagiotopoulos, C., Charrière, B., Van Wambeke, F., 2008. Distribution and bacterial availability of dissolved neutral sugars in the South East Pacific. Biogeosciences 5, 1165–1173.

Sempéré, R., Para, J., Tedetti, M., Charrière, B., Mallet, M., 2015. Variability of solar radiation and CDOM in surface coastal waters of the northwestern Mediterranean Sea. Photochem. Photobiol. 91, 851–861. https://doi.org/10.1111/php.12434.

Simmonet-Laprade, C., Budzinski, H., Babut, M., Le Menach, K., Munoz, G., Lauzent, M., Ferrari, B.J.D., Labadie, P., 2019. Investigation of the spatial variability of poly- and perfluoroalkyl substance trophic magnification in selected riverine ecosystems. Sci. Total Environ. 686, 393–401. https://doi.org/10.1016/j.scitotenv.2019.05.461.

Stahl, T., Mattern, D., Brunn, H., 2011. Toxicology of perfluorinated compounds. Environ. Sci. Eur. 23, 1–52. https://doi.org/10.1186/2190-4715-23-38.

Struglia, M.V., Mariotti, A., Filograsso, A., 2004. River discharge into the Mediterranean Sea: climatology and aspects of the observed variability. J. Clim. 17, 4740–4751. https://doi.org/10.1175/JCLI-3225.1.

Xia, J., Cao, Z., Peng, J., Fu, S., Fu, C., 2014. The use of spontaneous behavior, swimming performances and metabolic rate to evaluate toxicity of PFOS on topmouth gudgeon Pseudorasbora parva. Acta Ecol. Sin. 34, 284–289. https://doi.org/10.1016/J.CHNAES.2014.07.006.

Yohia, C., 2017. Genèse du mistral par interaction barocline et advection du tourbillon potentiel. Climatologie. https://doi.org/10.4267/climatologie.1182.

Zhang, L., Niu, J., Li, Y., Wang, Y., Sun, D., 2013. Evaluating the sub-lethal toxicity of PFOS and PFOA using rotifer Brachionus calyciflorus. Environ. Pollut. 180, 34–40. https://doi.org/10.1016/j.envpol.2013.04.031.